CHEMISTRY & CHEMICAL TECHNOLOGY

Chem. Chem. Technol., 2022, Vol. 16, No. 2, pp. 185–194

Chemistry

DFT STUDY OF SOME COPPER COMPLEXES AND THEIR DETECTION LIMITS

***Boulanouar Messaoudi**[1, 2]**, Tarik Attar**[1, 3, *]**, Naceur Benhadria**[1, 4]*

https://doi.org/10.23939/chcht16.02.185

Abstract. A theoretical investigation was probed to shed light on the correlation between low detection limit (LOD) in AdSV technique and metal trace complexes stability energy. The study was conducted by means of DFT calculations of copper traces complexation by using three different organic molecules as chelating agents, such as: morin, red pyrogallol and thymolphtalexone. The quantum chemistry calculations were carried out at the B3LYP/6-31G(d) level implemented in Gaussian 09 program package. The results of the electrophilicity index ω indicate that all the studied molecules have a tendency to exchange electron with copper. The negative values of free energy G and enthalpy H show that the complexation reactions are spontaneous in nature and exothermic. According to DFT calculations, copper-red pyrogallol complex with better detection limit (0.07 ng·mL^{-1}) has the lowest total energy (-5100.213 a.u.). Thus, there is a very strong relationship between the total energy of the three complexes and their detection limits in AdSV technique. Hence, the more stable complex has the better detection limit value.

Keywords: copper complex, detection limit, selectivity, Fukui indices, DFT calculations.

1. Introduction

Copper is a fundamental trace element and essential to support biological functions of human organism. It forms part of many copper-dependent enzymes and proteins joined to copper.[1] In human organism, copper shifts between the cuprous (Cu^{1+}) and cupric (Cu^{2+}) forms even though the most of the body's copper exists in the second oxidation form.[2]

Electrochemical methods offer many advantages compared to spectrometric and chromatographic methods, since the equipments are less expensive, faster, easier to be operated and the measurements can be carried out directly on site.[3] Moreover, spectroscopic methods analyze the total concentration of metal, while electrochemical techniques allow analysis of metals under different oxidation numbers. These techniques are founded on current measurement as a function of voltage.[4,5] The applications of various voltammetric analytical techniques cover many fields going from environment, chemical, medical, pharmaceutical, and food to metal industry. Among the electroanalytical methods used for the determination of ultra-trace elements, the adsorptive stripping voltammetry (AdSV) is considered as a powerful technique because of its wide linear dynamic range and low detection limit. The adsorptive stripping voltammetry can be analyzed at very low concentrations of organic and inorganic species.[6,7] The technique is based upon adsorptive accumulation of the analyte ions complexed with suitable ligands that are converted into stable complexes with adequate surface-active ligands to be adsorbed on the working electrode by means of a non-electrolytic process prior to the voltammetric scan.[8]

In literature, there are several reports on the application of adsorptive stripping voltammetry for the determination of trace metal, using different organic

---

[1] Higher School of Applied Sciences, P.O. Box 165 RP, Tlemcen, 13000, Algeria
[2] Laboratory of Applied Thermodynamics and Molecular Modeling, Department of Chemistry, University of Abou Bekr Belkaïd, B.P. 119, Tlemcen, 13000, Algeria
[3] Laboratory ToxicoMed, University of Abou Bekr Belkaïd, B.P.119, Tlemcen, 13000, Algeria
[4] Laboratory of Inorganic Materials Chemistry and Application, Department of Materials Engineering, University of Science and Technology of Oran (USTO M. B),
BP 1505, El M'naouar, 31000 Oran, Algeria
[*] *att_tarik@yahoo.fr*

substances as ligand such as chloranilic acid,[9-11] pyrogallol,[12] cupferron,[13] and calcon.[14]

In all literature reviews on electroanalysis, the concept of low detection limit (LOD) is one of the important parameters of any analytical method, which allows the comparison between different analytical techniques and choosing the most efficient and appropriate one for particular analytical task.[15] It is defined as the smallest concentration or absolute amount of analyte that has a signal significantly larger than the signal from a suitable blank.[16]

To the best of our knowledge, there have been only two works that showed the relationship between the limit of detection and the energy of stability by theoretical DFT calculations.[17,18] In the complex ion formation, there is a great change in the global energy between the ligand, metal and the metal complex. DFT method based on the quantum modeling is an important tool to understand the reason of best detection limit in electroanalysis. Therefore, based on experimental results,[19-21] our study is subdivided as follows. First, we have analyzed whether the experimental results are given under the same conditions by using AdSV technique. Among the parameters widely controlled in this technique, we can cite potential and time of adsorption. Secondly, we have conducted a DFT calculus of ligands, metal and complexes. Lastly, the LOD values given by AdSV technique for each metal are correlated with the results of DFT study.

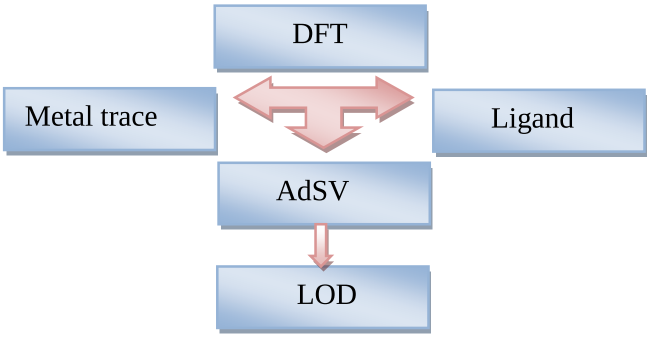

Scheme 1. Flowchart followed in the study

Thus, a theoretical study has been conducted to shed some light on the molecular and electronic structure of three organic molecules (morin, thymolphtalexone and red pyrogallol) and their corresponding complexes with copper ion. Our aim is to calculate several parameters to elucidate the importance of the relationship between the energy of stability of the complex and the detection limit in AdSV technique. A research methodology flowchart is given to clarify the steps that are followed in this study (Scheme 1).

2. Theoretical

2.1. Computational Details

Density Functional theoretical calculations at B3LYP/6-31G(d) level of theory[22-25] were used to study the energy stability of some organic molecules and their complexes with copper ion.[26] All calculations were done by using the Gaussian 09 program package.[27] Density functional theory (DFT) is a very successful computational quantum modeling method based on determining functionals that relate the electronic density to the energy. It is also used in several fields such as physics, chemistry and materials science to investigate the electronic structure of many species, in particular atoms, molecules, and condensed phases.

The full geometry optimizations followed by frequency calculations at the same level of theory were performed for all the stationary points. The Fukui indices were calculated using the finite difference approximation (FDA). We note that the cationic and anionic systems, required in the calculations of local indices, were kept at the same geometry of the neutral system. The electronic populations were computed using both MK (Merz-Singh-Kollman) and NPA (natural population analysis).[28]

2.2. Global Reactivity Indices

Rigorous definitions of popular qualitative chemical concepts such as electronegativity χ[29] and hardness η[30] have been given from the standpoint of conceptual density functional theory (DFT).[31,32] The electronegativity χ is defined as the negative quantity of chemical potential μ.[33,34] The physical expression is:

$$\chi = -\mu = -\left(\frac{\partial E}{\partial N}\right)_{\upsilon(r)} \tag{1}$$

where N is the number of electrons, E is the total energy and $\upsilon(r)$ is the external potential.

The hardness η is expressed as the first derivative of chemical potential as: [35]

$$\eta = \left(\frac{\partial^2 E}{\partial N^2}\right)_{\upsilon(r)} = \left(\frac{\partial \mu}{\partial N}\right)_{\upsilon(r)} \tag{2}$$

Using electron affinity (A) and ionisation potential (I), χ and η may be calculated as: [36,37]

$$\chi = \frac{1}{2}(I + A) \qquad (3)$$

$$\eta = \frac{1}{2}(I - A) \qquad (4)$$

According to Koopman's theorem, the frontier orbital energies $\varepsilon_{\mathrm{HOMO}}$ and $\varepsilon_{\mathrm{LUMO}}$ are related to the ionization potential I, and the electron affinity A by the following relations: [38]

$$A = -\varepsilon_{LUMO} \qquad (5)$$

$$I = -\varepsilon_{HOMO} \qquad (6)$$

By using the energies of the highest occupied $\varepsilon_{\mathrm{HOMO}}$ and lowest unoccupied molecular orbitals $\varepsilon_{\mathrm{LUMO}}$, the latter equations can be written as: [39]

$$\chi = -\frac{1}{2}(\varepsilon_{LUMO} + \varepsilon_{HOMO}) \qquad (7)$$

$$\eta = \frac{1}{2}(\varepsilon_{LUMO} - \varepsilon_{HOMO}) \qquad (8)$$

The electrophilicity index is calculated by the equation (7): [40]

$$\omega = \frac{\mu^2}{2\eta} \qquad (9)$$

This ratio is somehow a measure of the electrophilic power of a given system.

The nucleophilicity (N) of a molecule is defined as the negative value of the gas phase ionization potentials IP: [41]

$$N = -IP \qquad (10)$$

The nucleophilicity descriptor defined by Domingo's group by a practical expression is given as: [42]

$$N = \varepsilon_{HOMO(Nu)} - \varepsilon_{HOMO(TCE)} \qquad (11)$$

where $\varepsilon_{HOMO(TCE)}$ is the highest occupied molecular orbital energy of tetracyanoethylene (TCE) taken as a reference since it presents the lowest HOMO energy.[43]

2.3. Local Reactivity Indices

The reactivity of each site in a molecule toward a given attack is described by the local quantities. For instance, Fukui function is defined as: [44]

$$f(r) = \left[\frac{\partial \rho(r)}{\partial N}\right]_{\upsilon(r)} = \left[\frac{\delta \mu}{\delta \upsilon(r)}\right]_N \qquad (12)$$

where $\rho(r)$ is the electronic density of a system, N is the number of electrons and $\upsilon(r)$ is a constant external potential.

The condensed form of the Fukui function introduced by Yang and Mortier[45] can be calculated by the formulae:

For a nucleophilic attack

$$f_k^+ = [\rho_k(N+1) - \rho_k(N)] \qquad (13a)$$

For an electrophilic attack

$$f_k^- = [\rho_k(N) - \rho_k(N-1)] \qquad (13b)$$

Where $\rho_k(N)$, $\rho_k(N\text{-}1)$ and $\rho_k(N+1)$ are the gross electronic populations of the site k in neutral, cationic, and anionic systems, respectively.

The population analysis (Mulliken, natural, electrostatic, *etc.*) can be used to calculate the charges. The latter equations have been applied to a variety of systems in order to look for reactivity trends.[46,47]

3. Results and Discussion

Three molecules under study are of particular interest since they contain oxygen atoms as source of high electronic density. The complexation phenomenon on the metal surface (copper) is closely related to this heteroatom. The main goal of this research work is to show the ligands effect on the complexation mechanism in terms of stability of the formed complexes and find any possible relationship with the detection limit. In Fig. 1 the optimized structures of the three studied ligands are given.

In order to get more insight on the local reactivity, we have calculated the Fukui indices f_k^- using the labelling shown in Fig. 2.

The obtained results are presented in Tables 1, 2 and 3. The Fukui indexes, f_k^-, corresponding to electrophilic attack are calculated using two types of population analysis: Merz-Singh-Kollman (MK) and natural population analysis (NPA) in order to put in evidence the most reactive sites.

As it can be seen, the highest values of the local nucleophilicity indices (N_k) are attributed to oxygen atoms of morin, red pyrogallol and thymolphtalexone molecules at both populations used. For morin, atoms O25 and O32 are the most reactive sites with the highest N_k values at all. For red pyrogallol, either atoms O17 and O19 or O21 and O23 can form the complex since both couples are symmetrical. Indeed, for this molecule O25 is characterised by the highest value of N_k but it is not able to chelate with the metal atom due to the steric hindrance. For thymophtalexone, O31 and O43 present higher values than O12 and O13. However, the O31 and O43 are very far from each other and therefore the possibility of complexation is very weak and excluded. As a result, the oxygen (O) atoms of the three studied molecules are the most reactive centres. Consequently, this involves a greater ability to bind to the metal surface. Hence, the analysis, based on the static DFT-based indices, correctly predicts the regioselectivity observed for these complexes.

The distribution of electron density of frontier molecular orbitals of the three molecules is another key factor when dealing with reaction investigation. The HOMO (Fig. 3) density distribution is clearly scattered and bulky in the area containing the reactive oxygen atoms. In contrary, the HOMO-1 electronic distribution is somehow confusing since it covers almost all atoms and thus it does not give any clear response about the reactive region. Hence, the large electronic distribution on the oxygen atoms obviously shows that this region is a reactive centre where the transfer of electrons takes place from oxygen atoms of the three concerned ligands to the copper ion surface.

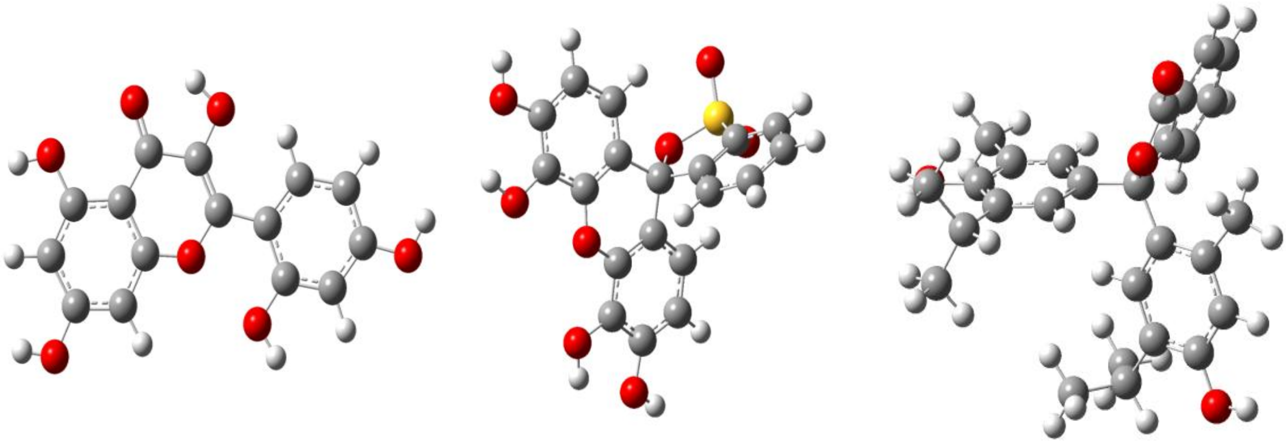

a) b) c)

Fig. 1. Molecular structures of morin (a), red pyrogallol (b) and thymolphtalexone (c)

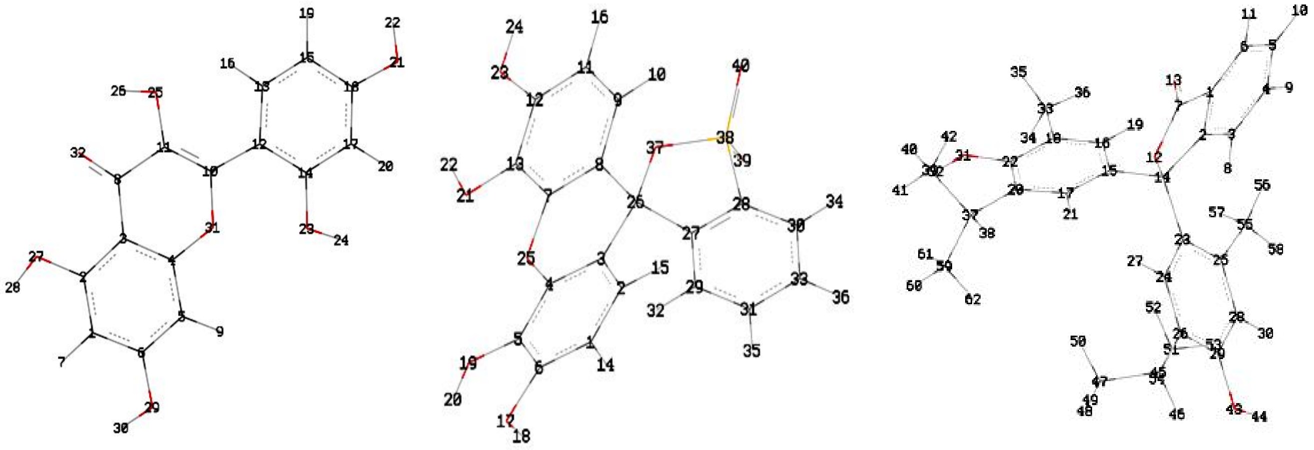

a) b) c)

Fig. 2. Atoms labelling for morin (a), red pyrogallol (b) and thymolphtalexone (c)

Table 1. Fukui (f^-) and DFT-based (N_k) indexes of the selected atoms for the morin using MK and NPA population analyses at B3LYP/6-31G(*d*) level of theory

Atom *k*	MK			NPA		
	f^+	f^-	N_k	f^+	f^-	N_k
O21	0.04321	0.06232	0.24816	-0.31638	0.39110	1.55731
O23	0.01226	0.01528	0.06083	-0.32547	0.36765	1.46394
O25	0.02789	0.09007	0.35865	-0.34026	0.47021	1.87232
O27	0.01589	0.03969	0.15804	-0.30513	0.34902	1.38975
O29	0.03629	0.03799	0.15126	-0.31740	0.35868	1.42822
O31	-0.00564	0.01390	0.05535	-0.19224	0.25921	1.03214
O32	0.10522	0.07446	0.29648	-0.16497	0.37081	1.47652

Table 2. Fukui (f^-) and DFT-based (N_k) indexes of the selected atoms for the red pyrogallol using MK and NPA population analyses at B3LYP/6-31G(*d*) level of theory

Atom *k*	MK			NPA		
	f^+	f^-	N_k	f^+	f^-	N_k
O17	0.02602	0.03024	0.10719	0.01755	0.02690	0.09534
O19	0.02816	0.06811	0.24139	0.01403	0.07088	0.25122
O21	0.02816	0.06811	0.24139	0.01403	0.07089	0.25126
O23	0.02603	0.03024	0.10717	0.01755	0.02690	0.09534
O25	-0.02831	0.01568	0.05559	0.00831	0.07703	0.27302
O37	0.04906	-0.01416	-0.05019	0.01761	-0.00150	-0.00532
S38	-0.02560	0.00847	0.03002	0.00584	-0.00343	-0.01216
O39	0.06076	0.02735	0.09695	0.04070	0.01839	0.06518
O40	0.06075	0.02736	0.09699	0.04071	0.01841	0.06525

Table 3. Fukui (f^-) and DFT-based (N_k) indexes of the selected atoms for the thymolphtalexone using MK and NPA population analyses at B3LYP/6-31G(*d*) level of theory

Atom *k*	MK			NPA		
	f^+	f^-	N_k	f^+	f^-	N_k
O12	-0.03513	0.01338	0.04441	0.03981	0.00189	0.00627
O13	0.09734	0.04896	0.16250	0.10117	0.04276	0.14193
O31	0.01319	0.05311	0.17629	0.01321	0.06732	0.22345
O43	0.01611	0.06567	0.21799	0.01498	0.06611	0.21944

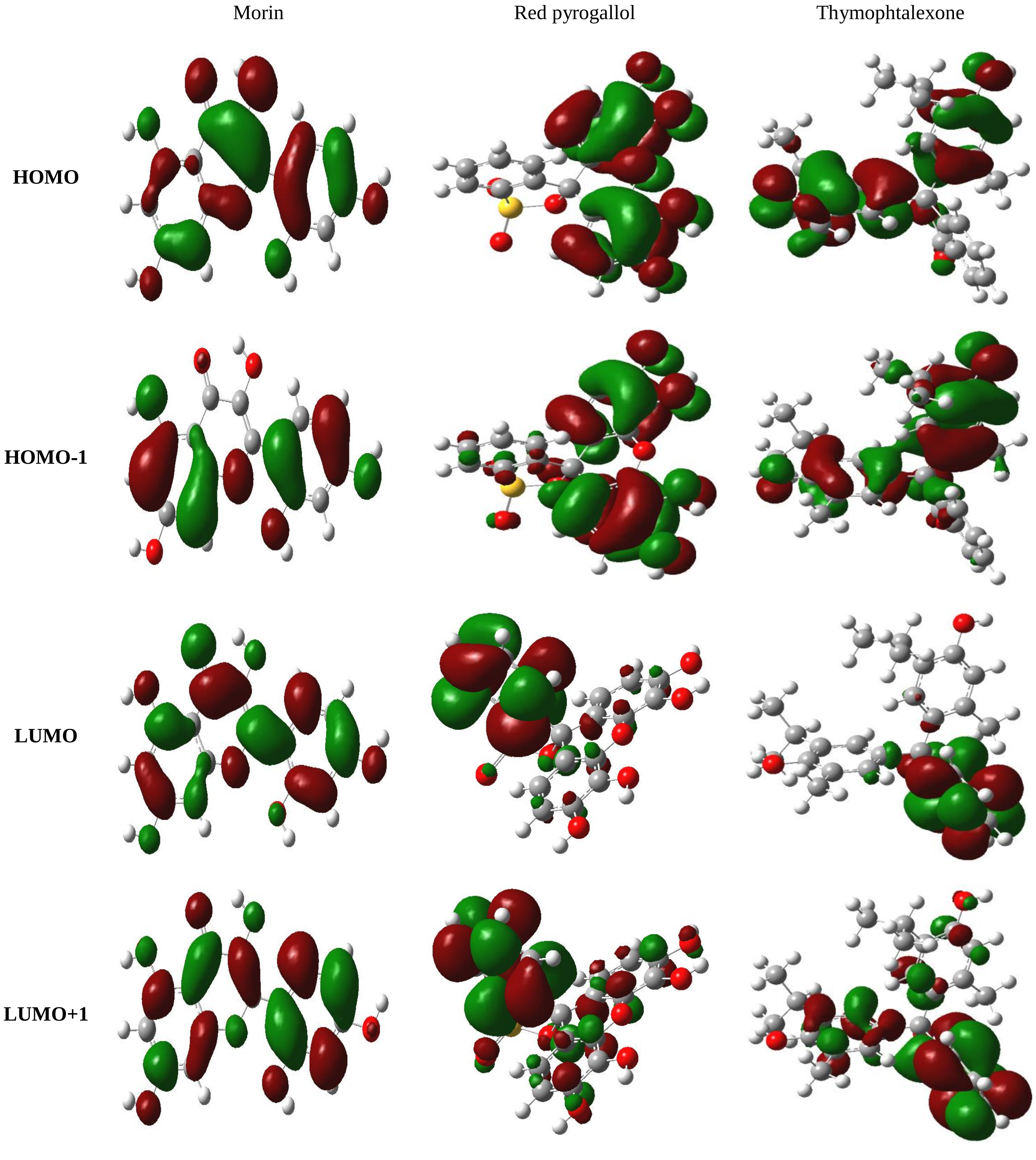

Fig. 3. Calculated HOMO, HOMO-1, LUMO and LUMO+1 molecular orbitals of the studied molecules at the B3LYP/6-31G(*d*) level of theory

HOMO and LUMO energies from Table 4 have been examined in order to find the tendency of each ligand to donate electrons (to empty molecular orbitals with low energy of convenient molecules), or to accept electrons, respectively. The resulting band gap ΔE $(E_{\mathrm{HOMO}} - E_{\mathrm{LUMO}})$ can be used to provide useful information on the chemical reactivity and kinetic stability of each ligand.[48,49] The band gap between the HOMO and LUMO orbitals energy has been found to increase in the order: morin < red pyrogallol < thermophtalexone (Table 4). Consequently, according to the obtained values of ΔE, morin presents the lowest reactivity, followed by red pyrogallol and thermophtalexone. In experimental point of view, the possible way of enhancing the adsorptive process and the sensitivity of the method is the use of adequate substituents which can change the stability of the complex, the net charge, and the solubility of the ligand and the complex as well. On the other hand, the sulfonate derivative is soluble in water and is more useful for analytical purposes.[50] Hence, the chemical reactivity of red pyrogallol is more adequate in this process.

The electronegativity χ has been proven to be a useful parameter in chemical reactivity theory. For instance, when copper and morin are joined together, electrons will flow from the entity having lower χ value (morin) to the one with higher χ value (Cu) until the equalization of chemical potentials. Actually, the red pyrogallol presents a medium χ value of 3.35 eV with respect to the two other substrates, 3.24 eV for morin and the value of 3.52 eV for thymolphtalexone (Table 4).

Moreover, the electrophilicity index ω gives indication whether a molecule has tendency to exchange electron(s). It is worthy to note here (see Table 4) that the studied molecules show electrophilicity values of 2.77, 2.71 and 2.52 eV for morin, thymolphtalexone and red pyrogallol, respectively. Therefore, the unoccupied ***d***-orbitals of copper atom can accept electrons from these molecules to form a coordinate bond. Theoretically speaking, these molecules can exchange electrons with copper atom *via* its anti-bonding orbitals to form a back-donating bond. Donation and back-donation processes strengthen the interaction of organic molecules with the metal ion. From the analysis given above, we can see that both the theoretical and experimental trends.

Table 4. HOMO and LUMO energies, global reactivity indices μ, η, ω, N, χ *and Gap* for the three studied compounds B3LYP/6-31G(*d*) level of theory

Substrate	HOMO, a.u.	LUMO, a.u.	μ, a.u.	η, a.u.	ω (eV)	N (eV)	χ (eV)	Gap (a.u.)
Morin	-0.18877	-0.04943	-0.1191	0.07	2.77	3.98	3.24	0.14
Red Pyrogallol	-0.20485	-0.04116	-0.1230	0.08	2.52	3.54	3.35	0.16
Thymolphtalexone	-0.21312	-0.04536	-0.1292	0.08	2.71	3.32	3.52	0.17

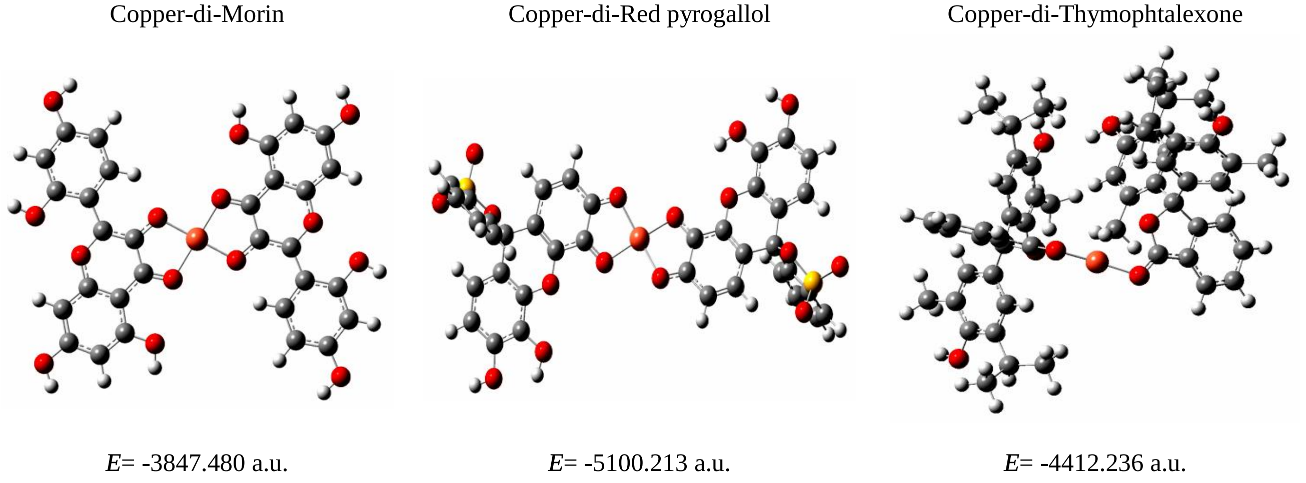

Fig. 4. Molecular structures of copper-morin, copper-red pyrogallol and copper-thymolphtalexone complexes at the B3LYP/6-31G(*d*) level of theory

The comparative study dealing with relative stabilities of the formed complexes, *i.e.* copper-morin, copper- red pyrogallol and copper-thymolphtalexone (Fig. 4) gives in all evidence a clear idea about the relationship between the detection limit and the complex stability. From the results presented in Fig. 4 and Table 5, we can see that copper-red pyrogallol complex presents the lowest values of both energy and free energy.

Basically, this means that this complex is more stable energetically and thermodynamically than the two other complexes. The thermodynamic parameters such as negative *G* values confirm the spontaneous nature and feasibility of the reaction process. The negative value of H strongly supports the exothermic nature of the reaction (Table 5).

The stability order finding is in good accordance with the detection limit order too, which is 0.07, 0.4 and 0.6 ng·mL^{-1} for copper-red pyrogallol,[19] copper-thymolphtalexone[20] and copper-morin,[21] respectively. Consequently, a stability/detection limit relationship could be established and we can conclude that the more stable the complex, the better its detection limit.

As it is indicated in Table 5, the entropy value of copper-thymolphtalexone complex is somehow larger than that of copper when bended to morin and red pyrogallol. Then, the former complex presents a high disorder with respect to the two left ones due to its important asymmetry. This puts in evidence that the stability of complexes depends on the nature of central atom and ligands.[51]

Table 5. Values of energy, enthalpy, free energy, and entropy calculated in the gas phase at B3LYP/6-31G(*d*) level of theory

	E, a.u.	*H*, a.u.	*G*, a.u.	S, J K^{-1} mol^{-1}
Cu^{2+}	-1640.172	-1640.170	-1640.189	166.009
Morin	-1104.145	-1103.897	-1103.959	546.895
Red pyrogallol	-1731.121	-1730.815	-1730.890	667.662
Thymolphtalexone	-1385.972	-1385.422	-1385.517	837.860
Complex morin	-3847.480	-3847.005	-3847.111	927.605
Complex red pyrogallol	-5100.213	-5099.644	-5099.777	1173.468
Complex thymolphtalexone	-4412.236	-4411.134	-4411.304	1499.972

4. Conclusions

The study looks for a relationship between the limit of detection of trace element in AdSV technique and the energetic stability of the formed complexes. Following this idea, we have performed some quantum chemical calculations at B3LYP/6-31G(*d*) level of theory on three organic molecules to investigate the structural and electronic properties and to elucidate the reactivity and selectivity of the molecules' centres. The results show that the main selective centre is oxygen (when bonding with copper) for all molecules. Since the oxygen O atom presents the highest electronic density, it can be easily favoured as a target for copper electrophilic attack. The electrophilic index values show that copper atom can accept electrons from organic molecules to form a coordinate bond. All the reactions of complexation are spontaneous and exothermic. The theoretical study at this level of theory revealed that chemical stabilities of complexes decrease in the order copper-red pyrogallol > copper-thymolphtalexone > copper-morin in line with experimental values of LOD. This finding can be familiarized to other complex systems used in AdSV technique.

Acknowledgements

The researcher team would like to express thanks to the Ministry of Higher Education and Scientific Research of the Algerian Government and Superior School of Applied Sciences for their fruitful support.

References

[1] Ilyechova, E.Y.; Bonaldi, E.; Orlov, I.A.; Skomorokhova, E.A.; Puchkova, L.V.; Broggini, M. CRISP-R/Cas9 Mediated Deletion of Copper Transport Genes CTR1 and DMT1 in NSCLC Cell Line H1299. Biological and Pharmacological Consequences. *Cell*. **2019**, *8*, 322. https://doi.org/10.3390/cells8040322

[2] Pahonțu, E.; Ilieș, D.-C.; Shova, S.; Paraschivescu, C.; Badea, M.; Gulea, A.; Roșu, T. Synthesis, Characterization, Crystal Structure and Antimicrobial Activity of Copper(II) Complexes with the Schiff Base Derived from 2-Hydroxy-4-Methoxybenzaldehyde. *Molecules* **2015**, *20*, 5771-5792. https://doi.org/10.3390/molecules20045771

[3] Attar, T., Medjati, N.D., Harek, Y., Larabi, L. Determination of Zinc levels in Healthy Adults from the West of Algeria by

Differential Pulse Anodic Stripping Voltammetry. *JAC* **2013**, *6,* 855-860. https://doi.org/10.24297/jac.v6i1.964

[4] Abu-Shandi, K.H. Catalytic Oxidation of Cyclohex-2-enol at Porous Iron Zeolite-like Material: Investigations by GC/MS, Polarography and X-ray Powder Diffraction. *Chem. Chem. Technol.* **2018**, *12*, 147-153. https://doi.org/10.23939/chcht12.02.147

[5] Attar, T.; Dennouni-Medjati, N.; Harek, Y.; Larabi, L. The Application of Differential Pulse Cathodic Stripping Voltammetry in the Determination of Trace Copper in Whole Blood. *J. Sens. Instrum*. **2013**, *1*, 31-38. https://doi.org/10.7726/jsi.2013.1003

[6] Attar, T.; Harek, Y.; Larabi, L. Determination of Copper in Whole Blood by Differential Pulse Adsorptive Stripping Voltammetry. Mediterr. *J. Chem*. **2014**, *2*, 691-700. https://doi.org/10.13171/mjc.2.6.2014.22.02.30

[7] Al-Rashdi, A.A.; Gahlan, A.A.; Farghaly, O.A. Selective Preconcentration of Ultra Trace Copper (II) ion Using Square Wave Cathodic Adsorptive Stripping Voltammetry at Modified Carbon Past Electrode. *Int. J. Electroche. Sci*. **2020**, *15*, 977-989. https://doi.org/10.20964/2020.01.83

[8] Attar, T.; Harek, Y.; Larabi, L. Determination of Ultra Trace Levels of Copper in Whole Blood by Adsorptive Stripping Voltammetry. *J. Korean. Chem. Soc*. **2013**, *57*, 568-573. https://doi.org/10.5012/jkcs.2013.57.5.568

[9] Sander, S. Simultaneous Adsorptive Stripping Voltammetric Determination of Molybdenum(VI), Uranium(VI), Vanadium(V), and Antimony(III). *Anal. Chim. Acta* **1999**, *394*, 81-89. https://doi.org/10.1016/S0003-2670(99)00218-4

[10] Bond, A.M.; Kratsis, S.K.; Newman, O.M.G. Combined Use of Differential Pulse Adsorptive and Anodic Stripping Techniques for the Determination of Antimony(III) and Antimony(V) in Zinc Electrolyte. *Anal. Chim. Acta* **1998**, *372*, 307-314. https://doi.org/10.1016/S0003-2670(98)00323-7

[11] Wagner, W.; Sander, S.; Henze, G. Trace Analysis of Antimony (III) and Antimony (V) by Adsorptive Stripping Voltammetry. *Fresenius J. Anal. Chem*. **1996**, *354*, 11-15. https://doi.org/10.1007/s002169600002

[12] Aguilar, J.C.; Rodríguez de San Miguel, E.; de Gyves, J. Adsorptive Stripping Voltammetry of In(III) in the Presence of Pyrogallol Red in Chloride-acetate Media. *Rev. Soc. Quím. Mex*. **2001**, *45*, 17-20.

[13] Grabarczyk, M.; Adamczyk, M. A Simple, Fast, and Inexpensive Simultaneous Determination of Trace Bismuth(III) and Lead(II) in Water Samples by Adsorptive Stripping Voltammetry. *J. Anal. Method. Chem*. **2017**, *2017*, 1. https://doi.org/10.1155/2017/1486497

[14] Deswati, D.; Suyani, H.; Safni, S.; Loekman, U.; Pardi, H. Simultaneous Determination of Cadmium, Copper and Lead in Sea Water by Adsorptive Stripping Voltammetry in the Presence of Calcon as a Complexing Agent. Indo. J. Chem., 2013, **13**, 236. https://doi.org/10.22146/ijc.21282

[15] Oleneva, E.; Khaydukova, M.; Ashina, J.; Yaroshenko, I.; Jahatspanian, I.; Legin, A.; Kirsanov, D. A Simple Procedure to Assess Limit of Detection for Multisensor Systems. *Sensors* **2019**, *19***,** 1359. https://doi.org/10.3390/s19061359

[16] Sanchez, J.M. Estimating Detection Limits in Chromatography from Calibration Data: Ordinary Least Squares Regression vs. Weighted Least Squares. *Separations* **2018**, *5*, 49. https://doi.org/10.3390/separations5040049

[17] Attar, T.; Messaoudi, B.; Benhadria, N. DFT Theoretical Study of Some Thiosemicarbazide Derivatives with Copper. *Chem. Chem. Technol.* **2020**, *14*, 20-25. https://doi.org/10.23939/chcht14.01.020

[18] Benhadria, N.; Attar, T.; Messaoudi, B. Understanding the Link Between the Detection Limit and the Energy Stability of Two Quercetin-Antimony Complexes by Means of Conceptual DFT. *S. Afr. J. Chem.* **2020**, *73*, 120-124. https://doi.org/10.17159/0379-4350/2020/v73a17

[19] Safavi, A.; Shams, E. Determination of Trace Amounts of Copper(II) by Adsorptive Stripping Voltammetry of its Complex with Pyrogallol Red. *Anal. Chim. Acta* **1999**, *385*, 265-272. https://doi.org/10.1016/S0003-2670(98)00580-7

[20] Babaei, A.; Babazadeh, M.; Shams, E. Simultaneous Determination of Iron, Copper, and Cadmium by Adsorptive Stripping Voltammetry in the Presence of Thymolphthalexone. *Electroanalysis* **2007**, *19*, 978-985. https://doi.org/10.1002/elan.200603812

[21] Hajian, R.; Shams, E. Application of Adsorptive Stripping Voltammetry to the Determination of Bismuth and Copper in the Presence of Morin. *Anal. Chim. Acta* **2003**, *491*, 63-69. https://doi.org/10.1016/S0003-2670(03)00789-X

[22] Calais, J.-L. Int. J. Density-functional theory of atoms and molecules. R.G. Parr and W. Yang, Oxford University Press, New York, Oxford, 1989. IX + 333 pp. Price £45.00. *Quantum Chem.* **1993**, *47*, 101. https://doi.org/10.1002/qua.560470107

[23] Perdew, J.P.; Burke, K.; Ernzerhof, M. Generalized Gradient Approximation Made Simple. *Rev. Lett*. **1996**, *77*, 3865. https://doi.org/10.1103/PhysRevLett.77.3865

[24] Voorhis T., Scuseria G.: Mol. Phys., 1997, **92,** 601. https://doi.org/10.1080/002689797170347

[25] Voorhis, T.V.; Scuseria, G.E. A Novel Form for the Exchange-correlation Energy Functional. *J. Chem. Phys.* **1998**, *109*, 400. https://doi.org/10.1063/1.476577

[26] Domingo, L.R.; Aurell, M.-J.; Perez, P.; Contreras, R. Quantitative Characterization of the Global Electrophilicity Power of Common Diene/dienophile Pairs in Diels–Alder Reactions. *Tetrahedron* **2002**, *58*, 4417-4423. https://doi.org/10.1016/S0040-4020(02)00410-6

[27] Frisch, M.J.; Trucks, G.W.; Schlegel, H.B.; Scuseria, G.E.; Robb, M.A.; Cheeseman, J.R. et al. *Gaussian 09, Revision A.02* ; Gaussian Inc.: Wallingford CT, 2009, 34.

[28] Besler, B.H.; Merz Jr, K.M.; Kollman, P.A. Atomic Charges Derived from Semiempirical Methods. *J. Comput. Chem.* **1990**, *11*, 431-439. https://doi.org/10.1002/jcc.540110404

[29] *Electronegativity, Structure and Bonding, Vol.* 66; Sen, K.; Jorgenson, C., Eds.; Springer Verlag: Berlin, Heidelberg, New York, London, Paris, Tokyo, 1987.

[30] Pal, S.; Roy, R.; Chandra, A.K. Change of Hardness and Chemical Potential in Chemical Binding: A Quantitative Model. *J. Phys. Chem*. **1994**, *98*, 2314-2317. https://doi.org/10.1021/j100060a018

[31] Parr, R.G.; von Szentpaly, L.; Liu, S. Electrophilicity Index. *J. Am. Chem. Soc.* **1999**, *121*, 1922-1924. https://doi.org/10.1021/ja983494x

[32] Geerlings, P.; De Proft, F.; Langenaeker, W. Conceptual Density Functional Theory. *Chem. Rev.* **2003**, *103*, 1793-1874. https://doi.org/10.1021/cr990029p

[33] Parr, R.G.; Donnelly, R.A.; Levy, M.; Palke, W.E. Electronegativity: The Density Functional Viewpoint. *J. Chem. Phys.* **1978**, *68*, 3801. https://doi.org/10.1063/1.436185

[34] Kohn, W.; Sham, L.G. Self-Consistent Equations Including Exchange and Correlation Effects. *J. Phys. Rev.* **1965**, *140*, A1133. https://doi.org/10.1103/PhysRev.140.A1133

[35] Parr, R.G.; Pearson, R.G. Absolute Hardness: Companion Parameter to Absolute Electronegativity. *J. Am. Chem. Soc.* **1983**, *105*, 7512-7516. https://doi.org/10.1021/ja00364a005

[36] Pearson, R.G. Absolute Electronegativity and Hardness: Application to Inorganic Chemistry. *Inorg. Chem.* **1988**, *27*, 734-740. https://doi.org/10.1021/ic00277a030

[37] Attar, T.; Benchadli, A.; Messaoudi, B.; Benhadria, N.; Choukchou-Braham, E. Experimental and Theoretical Studies of Eosin Y Dye as Corrosion Inhibitors for Carbon Steel in Perchloric Acid Solution. *Bull. Chem. React. Eng. Catal*. **2020**, *15*, 454-464. https://doi.org/10.9767/bcrec.15.2.7753.454-464

[38] Chygyrynets, E.; Vorobyova, V. A Study of Rape-Cake Extract as Eco-Friendly Vapor Phase Corrosion Inhibitor. *Chem. Chem. Technol*. **2014**, *8*, 235-242. https://doi.org/10.23939/chcht08.02.235

[39] Koopmans, T. Über die Zuordnung von Wellenfunktionen und Eigenwerten zu den Einzelnen Elektronen Eines Atoms. *Physica*. **1933**, *1*, 104-113. https://doi.org/10.1016/S0031-8914(34)90011-2

[40] Samsonowicz, M.; Regulska, E.; Świsłocka, R.; Butarewicz, A. Molecular Structure and Microbiological Activity of Alkali Metal 3,4-Dihydroxyphenylacetates. *J. Saudi Chem. Soc.* **2018**, *22*, 896-907. https://doi.org/10.1016/j.jscs.2018.01.009

[41] Jaramillo, P.; Domingo, L.R.; Chamorro, E.; Pérez, P. A Further Exploration of a Nucleophilicity Index Based on the Gas-phase Ionization Potentials. *J. Mol. Struct. Theochem* **2008**, *865*, 68-72. https://doi.org/10.1016/j.theochem.2008.06.022

[42] Contreras, R.; Andres J.; Safont, V.S.; Campodonico, P.; Santos, J.G. A Theoretical Study on the Relationship between Nucleophilicity and Ionization Potentials in Solution Phase. *J. Phys. Chem. A.* **2003**, *107*, 5588-5593. https://doi.org/10.1021/jp0302865

[43] Zhang, K.; Zhou, X.; Du, P.; Zhang, T.; Cai, M.; Sun, P.; Huang, C.-H.Oxidation of β-Lactam Antibiotics by Peracetic Acid: Reaction Kinetics, Product and Pathway Evaluation. *Water. Res.* **2017**, *123*, 153-161. https://doi.org/10.1016/j.watres.2017.06.057

[44] Parr, R.G.; Yang, W. Density Functional Approach to the Frontier-electron Theory of Chemical Reactivity. *J. Am. Chem. Soc*. **1984**, *106*, 4049-4050. https://doi.org/10.1021/ja00326a036

[45] Yang, W.; Mortier, W.J. The Use of Global and Local Molecular Parameters for the Analysis of the Gas-phase Basicity of Amines. *J. Am. Chem. Soc*. **1986**, *108*, 5708-5711. https://doi.org/10.1021/ja00279a008

[46] De Proft, F.; Martin, J.M.L.; Geerlings, P. Calculation of Molecular Electrostatic Potentials and Fukui Functions Using Density Functional Methods. *Chem. Phys. Lett.* **1996**, *256*, 400-408. https://doi.org/10.1016/0009-2614(96)00469-1

[47] Nguyen, L.T.; Le, T.N.; De Proft, F.; Chandra, A.K.; Langenaeker, W.; Nguyen, M.T.; Geerlings, P. Mechanism of [2 + 1] Cycloadditions of Hydrogen Isocyanide to Alkynes: Molecular Orbital and Density Functional Theory Study. *J. Am. Chem. Soc.* **1999**, *121*, 5992-6001. https://doi.org/10.1021/ja983394r

[48] Alam, M.J.; Ahmad, S. Anharmonic Vibrational Studies of l-Aspartic Acid Using HF and DFT Calculations. *Spectrochim. Acta A* **2012**, *96*, 992-1004. https://doi.org/10.1016/j.saa.2012.07.135

[49] Demir, P.; Akman, F. Molecular Structure, Spectroscopic Characterization, HOMO and LUMO Analysis of PU and PCL Grafted onto PEMA-co-PHEMA with DFT Quantum Chemical Calculations. *J. Mol. Struct.* **2017**, *1134*, 404-415. https://doi.org/10.1016/j.molstruc.2016.12.101

[50] Kopacz, M. Quercetin- and Morinsulfonates as Analytical Reagents. *J. Anal. Chem*. **2003**, *58*, 225-229. https://doi.org/10.1023/A:1022630319311

[51] Rakitskaya T., Truba A., Radchenko E.; Golub, A. *et al*.: Mono- and Bimetallic Complexes of Mn(II), Co(II), Cu(II), and Zn(II) with Schiff Bases Immobilized on Nanosilica as Catalysts in Ozone Decomposition Reaction. *Chem. Chem. Technol.* **2018**, *12*, 1-6. https://doi.org/10.23939/chcht12.01.001

Received: February 25, 2020 / Revised: April 10, 2020 / Accepted: September 12, 2020

ДФТ ДОСЛІДЖЕННЯ ДЕЯКИХ МІДНИХ КОМПЛЕКСІВ ТА ЇХ МЕЖА ВИЯВЛЕННЯ

Анотація. *Проведено теоретичне дослідження кореляції між низькою межею виявлення (LOD) методу адсорбційної вольтамперометрії (AdSV) та енергією стабільності комплексів металічних елементів. За допомогою DFT-розрахунків досліджено комплексоутворення мікроелементів міді з використанням як хелатоутворюючих речовин трьох органічних молекул: морин, червоний пірогалол та тимолфталексон. Проведено квантово-хімічні розрахунки на рівні B3LYP/6-31G(d), реалізовані в програмному пакеті Gaussian 09. Одержана величина індексу електрофільності ω вказує на те, що всі досліджувані молекули мають тенденцію до обміну електроном з міддю. Негативні значення вільної енергії G та ентальпії H показують, що реакції комплексоутворення мають спонтанний характер і є екзотермічними. Згідно з DFT розрахунками встановлено, що комплекс мідь-червоний пірогалол з більш ефективною межею виявлення (0,07 нг·мл*$^{-1}$*) має найменшу загальну енергію (-5100,213 a.u). Доведена залежність між загальною енергією трьох комплексів та межами їх виявлення за методом AdSV. Чим стабільніший комплекс, тим краще граничне значення виявлення.*

Ключові слова: *мідний комплекс, межа виявлення, селективність, індекси Фукуї, DFT розрахунки.*